Intraindividual Comparison of ^{18}F-PSMA-1007 PET/CT, Multiparametric MRI, and Radical Prostatectomy Specimens in Patients with Primary Prostate Cancer: A Retrospective, Proof-of-Concept Study

Claudia Kesch[1], Maria Vinsensia[2], Jan P. Radtke[1,3], Heinz P. Schlemmer[3], Martina Heller[4], Elena Ellert[5], Tim Holland-Letz[6], Stefan Duensing[1,4], Nils Grabe[7,8], Ali Afshar-Oromieh[2], Kathrin Wieczorek[5], Martin Schäfer[9], Oliver C. Neels[9], Jens Cardinale[9], Clemens Kratochwil[2], Markus Hohenfellner[1], Klaus Kopka[9,10], Uwe Haberkorn[2,11], Boris A. Hadaschik[1,12], and Frederik L. Giesel[2,10]

[1]Department of Urology, University Hospital Heidelberg, Heidelberg, Germany; [2]Department of Nuclear Medicine, University Hospital Heidelberg, Heidelberg, Germany; [3]Division of Radiology, German Cancer Research Center (dkfz), Heidelberg, Germany; [4]Section of Molecular Urooncology, Department of Urology, University of Heidelberg School of Medicine, Medical Faculty Heidelberg, Heidelberg, Germany; [5]Institute of Pathology, University Hospital Heidelberg, Heidelberg, Germany; [6]Division of Biostatistics, German Cancer Research Center (dkfz), Heidelberg, Germany; [7]Department of Medical Oncology, National Center for Tumor Diseases (NCT), University Hospital Heidelberg, Heidelberg, Germany; [8]Hamamatsu Tissue Imaging and Analysis Center, University of Heidelberg, Heidelberg, Germany; [9]Division of Radiopharmaceutical Chemistry, German Cancer Research Center (dkfz), Heidelberg, Germany; [10]German Cancer Consortium (DKTK), Heidelberg, Germany; [11]Clinical Cooperation Unit Nuclear Medicine, German Cancer Research Center (dkfz), Heidelberg, Germany; and [12]Department of Urology, University Hospital Essen, Essen, Germany

^{68}Ga-prostate-specific membrane antigen (PSMA)-11 PET/CT represents an advanced method for the staging of primary prostate cancer (PCa) and diagnosis of recurrent or metastatic PCa. However, because of the narrow availability of ^{68}Ga the development of alternative tracers is of high interest. The objective of this study was to examine the value of the new PET tracer ^{18}F-PSMA-1007 for the staging of local disease by comparing it with multiparametric MRI (mpMRI) and radical prostatectomy (RP) histopathology. **Methods:** In 2016, ^{18}F-PSMA-1007 PET/CT was performed in 10 men with biopsy-confirmed high-risk PCa. Nine patients underwent mpMRI in the process of primary diagnosis. Consecutively, RP was performed in all 10 men. Agreement analysis was performed retrospectively. PSMA staining was added for representative sections in RP specimen slices. Localization and agreement analysis of ^{18}F-PSMA-1007 PET/CT, mpMRI, and RP specimens was performed by dividing the prostate into 38 sections as described in the prostate imaging reporting and data system (PI-RADS) (version 2). Sensitivity, specificity, positive predictive values, negative predictive values (NPVs), and accuracy were calculated for total and near-total agreement. **Results:** ^{18}F-PSMA-1007 PET/CT had an NPV of 68% and an accuracy of 75%, and mpMRI had an NPV of 88% and an accuracy of 73% for total agreement. Near-total agreement analysis resulted in an NPV of 91% and an accuracy of 93% for ^{18}F-PSMA-1007 PET/CT and 91% and 87% for mpMRI, respectively. Retrospective combination of mpMRI and PET/CT had an accuracy of 81% for total and 93% for near-total agreement. **Conclusion:** Comparison with RP histopathology demonstrates that ^{18}F-PSMA-1007 PET/CT is promising for accurate local staging of PCa.

Key Words: ^{18}F-PSMA; PSMA-1007; prostate cancer; PET/CT; mpMRI
J Nucl Med 2017; 58:1805–1810
DOI: 10.2967/jnumed.116.189233

For men with primary or recurrent prostate cancer (PCa), accurate staging is essential for further therapy planning. Moreover, some therapeutic options such as focal therapy or nerve sparing radical prostatectomy (RP) require detailed information about the local T stage. Full-body bone scanning and cross-sectional abdominopelvic imaging for metastatic screening and multiparametric MRI (mpMRI) for local staging are recommended in patients with newly diagnosed high-risk PCa (*1*). mpMRI, in combination with fusion biopsy, has gained a key role for intraprostatic tumor localization and PCa diagnosis. In their recently published prostate MR imaging study (level 1b evidence) comparing mpMRI and conventional transrectal ultrasound biopsy with template prostate mapping biopsy, Ahmed et al. reported a sensitivity of up to 93%, a specificity of up to 41%, and a negative predictive value (NPV) of up to 89% for mpMRI (*2*). Comparisons with RP specimens have shown similar results (*3,4*), making mpMRI an established instrument for local T staging. However, the pooled sensitivity and the pooled specificity for lymph node staging with MRI are only 39% and 82%, respectively, making it an insufficient tool to reliably identify lymphatic spread (*5*).

In the attempt to find a 1-stop solution for both metastatic screening and local staging, these imaging techniques have been challenged by prostate-specific membrane antigen (PSMA) PET (*6,7*). PSMA is a membrane-bound enzyme with high expression

Received Dec. 28, 2016; revision accepted Apr. 19, 2017.
For correspondence or reprints contact: Frederik L. Giesel, Department of Nuclear Medicine, University Hospital Heidelberg, Im Neuenheimer Feld 400, 69120 Heidelberg, Germany.
E-mail: frederik@egiesel.com
Published online May 4, 2017.

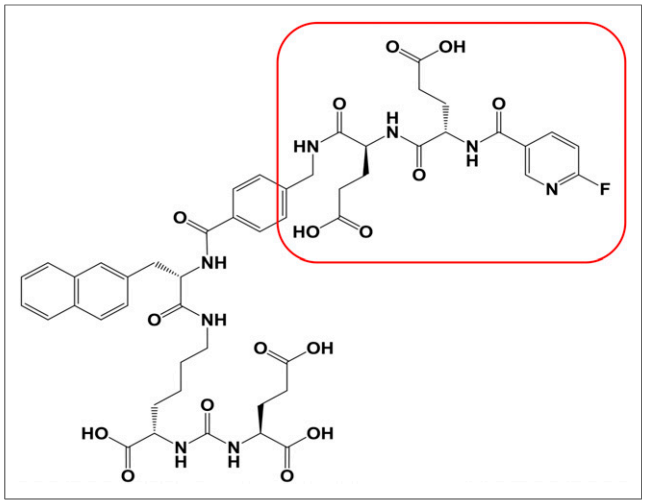

FIGURE 1. Chemical structure of PET tracer ^{18}F-PSMA-1007 with its radiolabel-bearing moiety marked in red.

in PCa cells and low expression in benign prostatic tissue (*8*), making it a promising target for PCa imaging. Specific inhibitors can bind to the catalytic site of PSMA, located in an extracellular domain, and are internalized after ligand binding (*9*). Small-molecule PSMA inhibitors have been designed for radiolabeling with several radionuclides including ^{68}Ga (*10,11*), ^{18}F (*12,13*), ^{89}Zr (*14*), and ^{99m}Tc (*15*), with ^{68}Ga-PSMA PET being the most commonly clinically used to date. ^{68}Ga-PSMA PET can detect metastatic tumor foci in patients with biochemical recurrence even at low prostate-specific antigen levels (*7*). In primary metastatic disease, ^{68}Ga-PSMA PET has been shown to detect metastases with high tumor-to-nontumor contrast and is therefore a useful tool for preoperative lymph node staging (*16*). To date, only a small number of studies examined ^{68}Ga-PSMA PET as a primary T staging modality. Nevertheless, promising results with a sensitivity ranging from 49% to 92% and a specificity from 92% to 94% have been shown (*17–21*). Any new PSMA radioligands need to be evaluated preclinically and clinically, if they can meet these excellent results. The novel PET tracer ^{18}F-PSMA-1007 (Fig. 1) (*22–25*) does have some advantageous characteristics that make it a promising candidate to compete with or even outperform ^{68}Ga-PSMA PET: with PET radiopharmacies connected to an on-site cyclotron, ^{18}F-PSMA-1007 can be produced in large scales. Furthermore, ^{18}F-PSMA-1007 is primarily eliminated via the hepatobiliary excretion route because of its moderate lipophilic characteristics. Therefore, almost no bladder activity occurs, providing ideal conditions for the evaluation of the prostate bed. It also has a low positron energy, which contingently offers better image quality (*26*), and its 110-min half-life may even allow transportation to satellite nuclear medicine centers. The aim of this study was to compare the utility of ^{18}F-PSMA-1007 PET/CT for T staging using RP specimens and mpMRI as reference.

MATERIALS AND METHODS

Study Population

Ten men with primary high-risk PCa underwent preoperative ^{18}F-PSMA-1007 PET/CT. Nine of these men were diagnosed with MRI/transrectal ultrasound (TRUS)–guided fusion biopsy and 1 with conventional TRUS biopsy. ^{18}F-PSMA-1007 was produced according to the German Pharmaceuticals Act §13(2b). Consecutive RP with extended pelvic lymphadenectomy was performed in all men as part of a multimodal treatment approach. Detailed patient characteristics and RP results are listed in Table 1.

The examinations were conducted in accordance with the Helsinki Declaration and our national regulations. The institutional review

TABLE 1
Patient Characteristics

Patient no.	Age (y)	iPSA (ng/mL)	Prostate volume (mL)	Days from mpMRI to surgery	Days from PSMA PET/CT to surgery	Histopathology TNM staging	Gleason-score/WHO group	Tumor volume (percentage of the whole prostate)	PCa SUV_{max} (1 h after injection)	PCa SUV_{max} (3 h after injection)	Normal tissue SUV_{max}
1	77	40.0	50	54	21	pT3b, pN1(4/14), L1, V0, Pn1, R1	4 + 5 = 9/5	30%	54.9	76.2	2.8
2	55	14.0	66	97	38	pT3b, pN1(5/40), L1, V0, Pn1, R1	4 + 5 = 9/5	45%	10.9	14.8	NA
3	65	13.9	52	193	56	pT3b, pN1(1/41), L0, V0, Pn1, RX	4 + 5 = 9/5	10%	24.3	30.2	2.7
4	64	10.0	40	116	1	pT3b, pN1(3/48), L1, V0, Pn1, R1	4 + 5 = 9/5	35%	18.9	27.5	2.9
5	64	12.2	23	66	19	pT3a, pN1(3/57), L1, V1, Pn1, R1	4 + 3 = 7b/3	10%	13.0	22.6	2.9
6	62	8.5	26	73	3	pT3a, pN0(0/21), L0, V0, Pn1, R1	3 + 4 = 7a/2	15%	15.5	27.5	3.6
7	69	5.8	50	147	26	pT3a, pN0(0/32), L0, V0, Pn0, R0	4 + 5 = 9/5	15%	36.7	58.6	3.0
8	73	31.0	47	——	6	pT3a, pN0(0/27), L0, V0, Pn1, R1	3 + 4 = 7a/2	30%	16.3	19.6	3.5
9	76	16.8	100	105	21	pT2c, pN1(3/40), L1, V0, Pn1, R0	4 + 5 = 9/5	20%	10.6	——	2.5
10	72	11.2	49	61	26	pT3b, pN1(5/61), L1, V0, Pn1, R1	4 + 5 = 9/5	70%	15.5	20.3	NA

iPSA = initial PSA; WHO = World Health Organization; NA = not applicable.

board approved this study (permit S-321), and all subjects signed a written informed consent form. In accordance with good practice in research, we disclose that other aspects (i.e., biodistribution and radiation dosimetry) of the study population have been published previously (*23*).

PET/CT Imaging

^{18}F-PSMA-1007 was synthesized as described previously (*22*). Scans were obtained on a Biograph mCT FlowScanner (Siemens). Unenhanced low-dose attenuation-correction CT (≈1.4 mSv) was performed 1 and 3 h after tracer injection in 9 patients. Because of noncompliance, 1 patient did not undergo the second-time-point PET/CT scan. CT scans was reconstructed with a slice thickness of 5 mm, an increment of 3–4 mm, a soft-tissue reconstruction kernel (B30), and Care Dose. PET was performed in 3-D FlowMotion (matrix, 200 × 200). Emission data were corrected for randoms, scatter, and decay. PET scans were reconstructed with an ordered-subset expectation maximization algorithm with 2 iterations and 21 subsets and Gauss-filtered to a transaxial resolution of 5 mm in full width at half maximum. Attenuation correction was performed using the low-dose CT data. Circular regions of interest were drawn around areas with focally increased uptake in transaxial slices and automatically adapted to a 3-dimensional volume of interest with e.soft software (Siemens) at a 50% isocontour to calculate the SUV.

mpMRI

Prebiopsy mpMRI was done on a 3-T (6 patients) or 1.5-T (3 patients) system without an endorectal coil including T2-weighted imaging, diffusion-weighted imaging, apparent diffusion coefficient map, and T1-weighted contrast-enhanced imaging. The median highest acquired b-value was 1,500 (range, 800–2,000). MRI examinations were performed at 6 different centers in a clinical setting. MRI studies were assessed by 2 readers: the first, a radiologist performing the mpMRI, and the second a well-experienced (>13 y) uroradiologist from our center. Reflecting clinical routine, the first radiologist assessing the MRI before prostate biopsy and PCa diagnosis was not masked to clinical data such as PSA and age. The second radiologist was masked to all data. Lesions with prostate imaging reporting and data system (PI-RADS; version 2) scores 4 or greater were considered positive in this study (*27*).

Histopathologic Analysis

In addition to the routine clinical evaluation of RP specimens by different pathologists according to standards of the International Society of Urological Pathology, a second histopathologic evaluation was performed under the supervision of 1 dedicated uropathologist masked to PET and MRI data (*28*). Tissue samples were provided by the tissue bank of the National Center for Tumor Diseases in accordance with the regulations of the tissue bank and ethics approval. Additional PSMA immunohistochemistry staining was performed for representative sections. Therefore, sections were first deparaffinized with xylene and then rehydrated in graded ethanol series. Antigens were retrieved under steam cooking using Target Retrieval Solution (Dako). The mouse monoclonal PSMA antibody clone 3E6 (Dako) was used, diluted 1:100, and incubated overnight at 4°C. Immunodetection was performed with a Histostain–Plus detection kit (Invitrogen) according to the manufacturer's recommendations. To generate digital whole-mount slide images, sections were scanned using a Nanozoomer 2.0-HT Scansystem (Hamamatsu Photonics).

Statistical Analysis

Patient demographics were analyzed descriptively. For tumor localization and agreement analysis, each prostate was divided into 3 axial levels (base, mid, apex) and divided at each level into 12 sections with 2 additional sections for the right and left seminal vesicle comparable with the scheme used in PI-RADS (version 2) (*27*). For each imaging modality (^{18}F-PSMA-1007 PET/CT and mpMRI) and for histopathology, the data for each patient were reported on a print of the 38-sector scheme, with each positive sector being marked by the expert uroradiologist, nuclear medicine physician, and uropathologist, respectively. Agreement and true positivity of the imaging modality with histopathology were considered if there was exactly the same region marked (total agreement) or if there was a discrepancy of up to 1 region in any direction (near-total agreement) (*4,21*). For the combination of ^{18}F-PSMA-1007 PET/CT and mpMRI, agreement was considered if either both or one of the methods was suggestive of tumor in this region. Sensitivity, specificity, positive predictive values (PPVs), NPVs, and accuracy were calculated for both total and near-total agreement. Analysis was performed using SPSS statistics (version 23; IBM Corp.). Data were reported according to the Standards for Reporting Diagnostic accuracy studies (STARD) (Supplemental Table 1; supplemental materials are available at http://jnm.snmjournals.org).

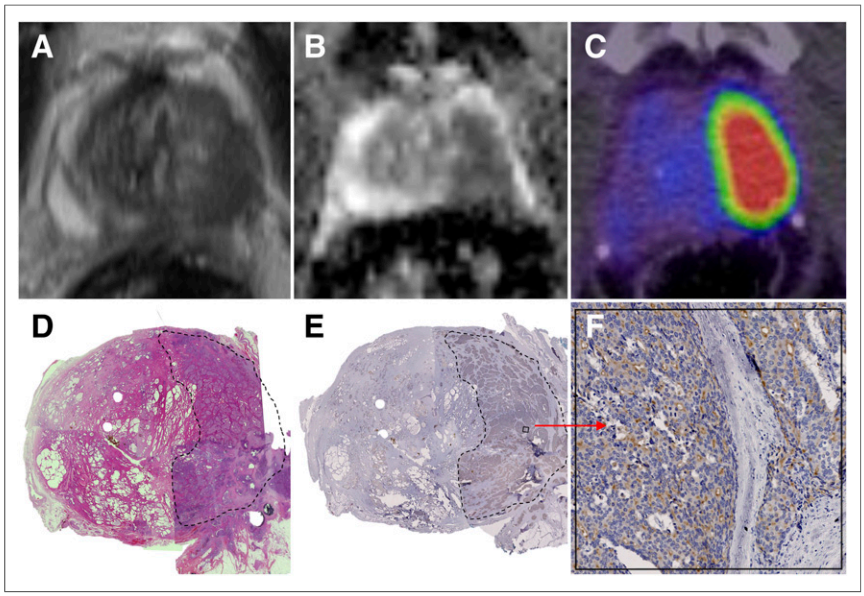

FIGURE 2. Correlation of MRI, ^{18}F-PSMA-1007 PET/CT, and histopathology. (A) T2-weighted MRI sequence. (B) Apparent diffusion coefficient map. (C) ^{18}F-PSMA-1007 PET/CT. (D) Hematoxylin and eosin staining. (E) PSMA staining. (F) PSMA staining with 30× zoom.

RESULTS

In total, 10 men were included in this retrospective analysis. The median age was 67 y (range, 62–77 y). Median initial PSA was 13.1 ng/mL (range, 5.8–40.0 ng/mL), with a median prostate volume of 49.5 mL (range, 23–100 mL). A median of 97 d (range, 54–193 d) passed from MRI and 21 d (range, 1–56 d) from PET to RP, respectively. Median SUV_{max} was 15.9 (range, 10.6–54.9) after 1 h and 27.5 (range, 14.8–76.2) after 3 h in the primary tumor. Patient characteristics are listed in Table 1. Overall ^{18}F-PSMA PET/CT, mpMRI, and final histopathology correlated well (Fig. 2). On a per-lesion basis, both imaging modalities detected the index lesion (biggest lesion) correctly, but ^{18}F-PSMA-1007 PET/CT missed 2 nonindex

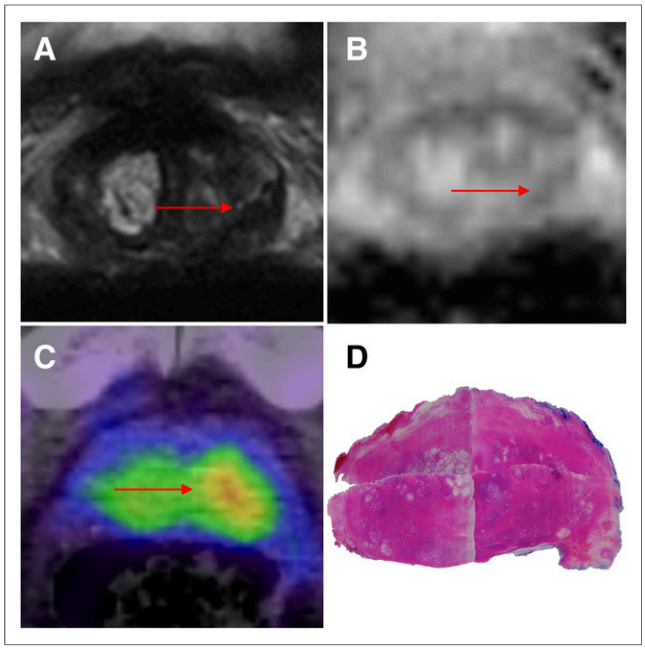

FIGURE 3. Example of false-positive lesions on MRI and ^{18}F-PSMA-1007 PET/CT. (A) T2-weighted MRI sequence, with false-positive lesion marked with red arrow. (B) Apparent diffusion coefficient map, with false-positive lesion marked with red arrow. (C) ^{18}F-PSMA-1007 PET/CT, with false-positive lesion marked with red arrow. (D) Hematoxylin and eosin staining without tumor lesions correlating with imaging modalities.

lesions detected in the histopathology specimen. Similarly, mpMRI missed 2 of the histopathologically confirmed nonindex lesions. ^{18}F-PSMA-1007 PET/CT showed 3 false-positive lesions and mpMRI 4 (Fig. 3). Only 4 of the 10 patients had obvious multifocality as most of the patients in this high-risk cohort had 1 big index lesion occupying a median of 25% (range, 10%–70%) of the prostate volume. Multifocality was correctly identified by ^{18}F-PSMA-1007 PET/CT in 2 cases (Fig. 4). mpMRI detected multifocality in 1 case, mentioning that only 3 patients undergoing mpMRI showed multifocality in the final histopathology.

A clear separation of bladder and prostate without any spillover from activity in the urine was possible in all patients, and transition zone PET signal was always confirmed with tumor tissue in pathology. In the final histopathology, 5 patients had seminal vesicle invasion (pT3b), which was missed in 1 case by MRI and in 1 case by PET. In the 38-sector analysis, mpMRI detected 113 of 188 histopathologically tumor-bearing regions, and ^{18}F-PSMA-1007 PET/CT detected 151 of 212.

^{18}F-PSMA-1007 PET/CT had a 71% sensitivity, 81% specificity, 83% PPV, 68% NPV, and 75% accuracy for total agreement and 93% sensitivity, 92% specificity, 94% PPV, 91% NPV, and 93% accuracy for near-total agreement. mpMRI had an 86% sensitivity, 64% specificity, 60% PPV, 88% NPV, and 73% accuracy for total agreement and 92% sensitivity, 83% specificity, 85% PPV, 91% NPV, and 87% accuracy for near-total agreement. The combination of ^{18}F-PSMA-1007 PET/CT and mpMRI had 81% sensitivity, 81% specificity, 85% PPV, 75% NPV, and 81% accuracy for total agreement and 89% sensitivity, 99% specificity, 99% PPV, 85% NPV, and 93% accuracy for near-total agreement (Table 2).

PSMA staining was performed exemplarily in representative histopathology samples. Interestingly, intratumoural heterogeneity was observed because not all tumor-bearing cells within 1 lesion showed a positive PSMA signal (Figs. 2E and 2F).

DISCUSSION

^{18}F-PSMA-1007, a novel diagnostic PSMA ligand, demonstrated promising local T staging of PCa because of its favorable pharmacokinetics and tumor-specific uptake. In this study of 10 patients with high-risk PCa, ^{18}F-PSMA-1007 showed high sensitivity (71% for total and 93% for near-total agreement), specificity (81% for total and 92% for near-total agreement), and accuracy (75% for total and 93% for near-total agreement).

Considering the small patient cohort of this study, no disruption due to activity spillover from the urine such as that described for ^{68}Ga-PSMA-11 (*17,19*) was found. Moreover, because of its advantageous characteristics (high production capacity, longer physical half-life, and low positron emission energy (*26*)), our study suggests that ^{18}F-PSMA-1007 PET/CT can compete with ^{68}Ga-PSMA PET/CT for PCa T staging. Rhee et al. found a sensitivity of 49%, a specificity of 94%, a PPV of 81%, and an NPV of 88% when the ^{68}Ga-PSMA-11 PET/CT scans of 20 patients with localized PCa were compared with RP specimens using a 27-region model (*20*). For a 6-region model, Fendler et al. found a sensitivity of 67%, a specificity of 92%, a PPV of 97%, an NPV of 42%, and an accuracy of 86% for the detection of seminal vesicle involvement (*18*). These results are comparable with a ^{68}Ga-PSMA-11 PET/MRI study of Eiber et al. who describe a sensitivity of 64% and a specificity of 94% (*17*). The highest sensitivity was found by Rahbar et al. with 92%, a specificity of 92%, a PPV of 96%, and an NPV of 85% in a study including 6 patients and a 22-region model (*19*).

Recently, results of 2 other ^{18}F-based compounds have been described. *N*-[*N*-[(*S*)-1,3-dicarboxypropyl]carbamoyl]-4-^{18}F-fluorobenzyl-L-cysteine was evaluated by Rowe et al. in patients with PCa, but it performed less sensitively than MRI and resulted in a low tumor-to-background ratio due to high blood-pool activity (*29*). Thereupon, a second-generation equivalent, 2-(3-{1-carboxy-5-[(6-^{18}F-fluoro-pyridine-3-carbonyl)-amino]-pentyl}-ureido)-pentanedioic acid, has been developed, which has a stronger binding affinity, less blood-pool activity, and a reduced radiation exposure compared with its first-generation equivalent (*11,30*). However, this promising tracer is still lacking histopathologic validation.

Compared with mpMRI, ^{18}F-PSMA-1007 performed slightly better for near-total agreement regarding sensitivity, specificity,

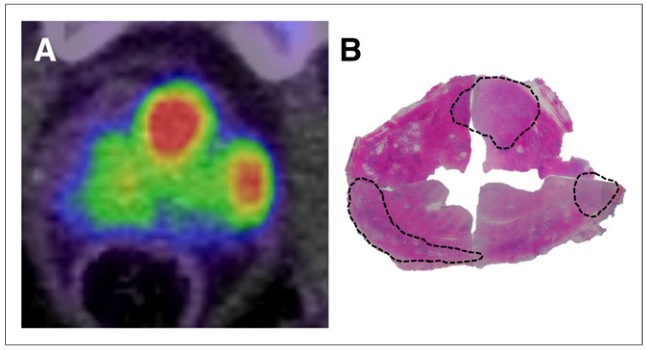

FIGURE 4. Multifocal tumor growth. (A) ^{18}F-PSMA PET/CT. (B) Hematoxylin and eosin staining.

TABLE 2
Sensitivity, Specificity, PPV, NPV, and Accuracy of ^{18}F-PSMA-1007 PET/CT and mpMRI Compared with RP Specimen Histopathology

Agreement	Sensitivity	Specificity	PPV	NPV	Accuracy
Total					
^{18}F-PSMA-1007 PET/CT	71% (64%–77%)	81% (75%–87%)	83% (77%–88%)	68% (61%–75%)	75%
mpMRI	86% (79%–92%)	64% (57%–71%)	60% (52%–67%)	88% (82%–93%)	73%
Combination	81% (75%–86%)	81% (73%–87%)	85% (79%–90%)	75% (68%–82%)	81%
Near-total					
^{18}F-PSMA-1007 PET/CT	93% (89%–96%)	92% (87%–96%)	94% (90%–97%)	91% (86%–95%)	93%
mpMRI	92% (87%–96%)	83% (76%–88%)	85% (79%–90%)	91% (85%–95%)	87%
Combination	89% (84%–93%)	99% (95%–100%)	99% (96%–100%)	85% (78%–90%)	93%

Data in parentheses are 95% CIs.

PPV, and accuracy but had a worse sensitivity and NPV for total agreement. This variance can be explained by the higher resolution and anatomic landmark definition derived from mpMRI. On the basis of per-lesion analysis, ^{18}F-PSMA-1007 PET/CT was superior to mpMRI, with both fewer false-negatives and fewer false-positives. Today, mpMRI in combination MRI/TRUS fusion biopsy outperforms the standard 12-core TRUS biopsy and plays therefore a pivotal role for PCa diagnosis and T staging (*2,31*). Compared with other data, our mpMRI results lie within the reported sensitivity of 63%–98%, NPV of 63%–98%, and specificity of 23%–87% (*32,33*). However, the recently published prostate MR imaging study by Ahmed et al. (*2*) reports a better sensitivity (96%) and NPV (92%) than the ones presented here of 86% and 88%, respectively. Despite the different reference tests (mapping biopsy vs. RP specimen) and different prevalence of high-risk disease, this demonstrates that careful interpretation of our data is necessary considering the long time span between mpMRI and surgery that appeared in our study (median, 97 d [range, 54–193 d]). Also, reflecting clinical routine at our institution, the men included in this retrospective study underwent mpMRI at 6 different centers lacking a common protocol. Thus, mpMRI scans varied between 3-T and 1.5-T and had different high b-values with a range of 800–2,000. Nevertheless, our results are consistent with other studies comparing the performance of ^{68}Ga-PSMA PET with mpMRI for local T staging (*17,20,21*). Rhee et al. (*20*), our group (*21*), and Eiber et al. (*17*) all found a slight advantage favoring ^{68}Ga-PSMA PET over mpMRI but similar to the present study the most promising results were achieved by combining the 2 methods, pointing in the direction of ^{18}F-PSMA-1007 PET/MRI as the future premium hybrid imaging modality.

One limitation of our study is given by its retrospective data analysis. A second limitation is in the nature of the study cohort itself in which only high-risk patients were examined. Accurate local T staging is of major importance for this group of patients as well, but it is of even more interest in intermediate-risk patients and in patients potentially harboring PCa with a suggestion of PCa to guide therapy or prostate biopsy. We know that high PSMA expression and therefore a strong PSMA PET/CT signal correlates with high Gleason scores (*7*). Hence, the transferability of our data and the utility of ^{18}F-PSMA-1007 PET in lower risk disease have yet to be assessed. A third limitation is the challenging comparability of imaging modalities and RP specimens due to organ slicing and shrinking artifacts during tissue preparation. We tried to overcome this limitation by use of sector schemes, near-total agreement analysis, and per-lesion analysis in addition to total agreement analysis.

CONCLUSION

The comparison with RP histopathology demonstrates that ^{18}F-PSMA-1007 PET/CT is a promising prostate imaging tool providing accurate T staging of PCa. Future studies should focus on the combination of ^{18}F-PSMA-1007 PET with MRI to achieve a higher resolution and anatomic landmark definition.

DISCLOSURE

Jens Cardinale, Martin Schäfer, Frederik L. Giesel, Uwe Haberkorn, and Klaus Kopka hold a patent application for PSMA-1007. No other potential conflict of interest relevant to this article was reported.

ACKNOWLEDGMENTS

We acknowledge Daniel Roth for graphic support as well as Viktoria Reiswich and Kirsten Kunze for image acquisition.

REFERENCES

1. Mottet N, Bellmunt J, Bolla M, et al. EAU–ESTRO–SIOG guidelines on prostate cancer: part 1—screening, diagnosis, and local treatment with curative intent. *Eur Urol.* 2017;71:618–629.
2. Ahmed HU, El-Shater Bosaily A, Brown LC, et al. Diagnostic accuracy of multiparametric MRI and TRUS biopsy in prostate cancer (PROMIS): a paired validating confirmatory study. *Lancet.* 2017;389:815–822.
3. Le JD, Tan N, Shkolyar E, et al. Multifocality and prostate cancer detection by multiparametric magnetic resonance imaging: correlation with whole-mount histopathology. *Eur Urol.* 2015;67:569–576.
4. Radtke JP, Schwab C, Wolf MB, et al. Multiparametric magnetic resonance Imaging (MRI) and MRI-transrectal ultrasound fusion biopsy for index tumor detection: correlation with radical prostatectomy specimen. *Eur Urol.* 2016;70: 846–853.
5. Hövels AM, Heesakkers RA, Adang EM, et al. The diagnostic accuracy of CT and MRI in the staging of pelvic lymph nodes in patients with prostate cancer: a meta-analysis. *Clin Radiol.* 2008;63:387–395.
6. Kratochwil C, Afshar-Oromieh A, Kopka K, Haberkorn U, Giesel FL. Current status of prostate-specific membrane antigen targeting in nuclear medicine: clinical translation of chelator containing prostate-specific membrane antigen ligands into diagnostics and therapy for prostate cancer. *Semin Nucl Med.* 2016;46:405–418.

7. Perera M, Papa N, Christidis D, et al. Sensitivity, specificity, and predictors of positive ^{68}Ga-prostate-specific membrane antigen positron emission tomography in advanced prostate cancer: a systematic review and meta-analysis. *Eur Urol.* 2016;70:926–937.
8. Kasperzyk JL, Finn SP, Flavin R, et al. Prostate-specific membrane antigen protein expression in tumor tissue and risk of lethal prostate cancer. *Cancer Epidemiol Biomarkers Prev.* 2013;22:2354–2363.
9. Eder M, Neels O, Müller M, et al. Novel preclinical and radiopharmaceutical aspects of [^{68}Ga]Ga-PSMA-HBED-CC: a new PET tracer for imaging of prostate cancer. *Pharmaceuticals.* 2014;7:779–796.
10. Afshar-Oromieh A, Avtzi E, Giesel FL, et al. The diagnostic value of PET/CT imaging with the ^{68}Ga-labelled PSMA ligand HBED-CC in the diagnosis of recurrent prostate cancer. *Eur J Nucl Med Mol Imaging.* 2015;42:197–209.
11. Eder M, Schäfer M, Bauder-Wüst U, et al. ^{68}Ga-complex lipophilicity and the targeting property of a urea-based PSMA inhibitor for PET imaging. *Bioconjug Chem.* 2012;23:688–697.
12. Szabo Z, Mena E, Rowe SP, et al. Initial evaluation of [^{18}F]DCFPyL for prostate-specific membrane antigen (PSMA)-targeted PET imaging of prostate cancer. *Mol Imaging Biol.* 2015;17:565–574.
13. Rowe SP, Macura KJ, Mena E, et al. PSMA-based [^{18}F]DCFPyL PET/CT is superior to conventional imaging for lesion detection in patients with metastatic prostate cancer. *Mol Imaging Biol.* 2016;18:411–419.
14. Pandit-Taskar N, O'Donoghue JA, Beylergil V, et al. ^{89}Zr-huJ591 immuno-PET imaging in patients with advanced metastatic prostate cancer. *Eur J Nucl Med Mol Imaging.* 2014;41:2093–2105.
15. Hillier SM, Maresca KP, Lu G, et al. ^{99m}Tc-labeled small-molecule inhibitors of prostate-specific membrane antigen for molecular imaging of prostate cancer. *J Nucl Med.* 2013;54:1369–1376.
16. Maurer T, Gschwend JE, Rauscher I, et al. Diagnostic efficacy of ^{68}Gallium-PSMA positron emission tomography compared to conventional imaging for lymph node staging of 130 consecutive patients with intermediate to high risk prostate cancer. *J Urol.* 2016;195:1436–1443.
17. Eiber M, Weirich G, Holzapfel K, et al. Simultaneous ^{68}Ga-PSMA HBED-CC PET/MRI improves the localization of primary prostate cancer. *Eur Urol.* 2016; 70:829–836.
18. Fendler WP, Schmidt DF, Wenter V, et al. ^{68}Ga-PSMA-HBED-CC PET/CT detects location and extent of primary prostate cancer. *J Nucl Med.* 2016;57:1720–1725.
19. Rahbar K, Weckesser M, Huss S, et al. Correlation of intraprostatic tumor extent with ^{68}Ga-PSMA distribution in patients with prostate cancer. *J Nucl Med.* 2016;57:563–567.
20. Rhee H, Thomas P, Shepherd B, et al. Prostate specific membrane antigen positron emission tomography may improve the diagnostic accuracy of multiparametric magnetic resonance imaging in localized prostate cancer. *J Urol.* 2016;196: 1261–1267.
21. Giesel FL, Sterzing F, Schlemmer HP, et al. Intra-individual comparison of ^{68}Ga-PSMA-11-PET/CT and multi-parametric MR for imaging of primary prostate cancer. *Eur J Nucl Med Mol Imaging.* 2016;43:1400–1406.
22. Cardinale J, Schäfer M, Benešová M, et al. Preclinical evaluation of [^{18}F]PSMA-1007: a new PSMA-ligand for prostate cancer imaging. *J Nucl Med.* 2017;58:425–431.
23. Giesel FL, Hadaschik B, Cardinale J, et al. F-18 labelled PSMA-1007: biodistribution, radiation dosimetry and histopathological validation of tumor lesions in prostate cancer patients. *Eur J Nucl Med Mol Imaging.* 2017;44:678–688.
24. Giesel FL, Cardinale J, Schäfer M, et al. ^{18}F-labelled PSMA-1007 shows similarity in structure, biodistribution and tumour uptake to the theragnostic compound PSMA-617. *Eur J Nucl Med Mol Imaging.* 2016;43:1929–1930.
25. Giesel FL, Kesch C, Yun M, et al. ^{18}F-PSMA-1007 PET/CT detects micrometastases in a patient with biochemically recurrent prostate cancer. *Clin Genitourin Cancer.* 2017;15:e497–e499.
26. Sanchez-Crespo A. Comparison of gallium-68 and fluorine-18 imaging characteristics in positron emission tomography. *Appl Radiat Isot.* 2013;76:55–62.
27. Barentsz JO, Weinreb JC, Verma S, et al. Synopsis of the PI-RADS v2 guidelines for multiparametric prostate magnetic resonance imaging and recommendations for use. *Eur Urol.* 2016;69:41–49.
28. van der Kwast TH, Amin MB, Billis A, et al. International Society of Urological Pathology (ISUP) Consensus Conference on handling and staging of radical prostatectomy specimens: working group 2—T2 substaging and prostate cancer volume. *Mod Pathol.* 2011;24:16–25.
29. Rowe SP, Gage KL, Faraj SF, et al. ^{18}F-DCFBC PET/CT for PSMA-based detection and characterization of primary prostate cancer. *J Nucl Med.* 2015;56: 1003–1010.
30. Li X, Rowe SP, Leal JP, et al. Quantiative parameters in PSMA-targeted PET imaging with ^{18}F-DCFPyL: variability in normal organ uptake. *J Nucl Med.* 2017;58:942–946.
31. Siddiqui MM, Rais-Bahrami S, Turkbey B, et al. Comparison of MR/ultrasound fusion-guided biopsy with ultrasound guided biopsy for the diagnosis of prostate cancer. *JAMA.* 2015;313:390–397.
32. Thompson JE, Moses D, Shnier R, et al. Multiparametric magnetic resonance imaging guided diagnostic biopsy detects significant prostate cancer and could reduce unnecessary biopsies and over detection: a prospective study. *J Urol.* 2014;192:67–74.
33. Fütterer JJ, Briganti A, De Visschere P, et al. Can clinically significant prostate cancer be detected with multiparametric magnetic resonance imaging? A systematic review of the literature. *Eur Urol.* 2015;68:1045–1053.